Robotics and Autonomous Systems 61 (2013) 775–784

Contents lists available at SciVerse ScienceDirect

Robotics and Autonomous Systems

journal homepage: www.elsevier.com/locate/robot

Bounded controllers for global path tracking control of unicycle-type mobile robots

K.D. Do

Department of Mechanical Engineering, Curtin University, Perth, WA 6845, Australia

HIGHLIGHTS

- Global path tracking controllers are designed for mobile robots.
- The new one-step ahead backstepping method is introduced to design bounded controllers.
- The control torques are bounded with a predefined bound for all initial conditions.
- The tracking errors globally asymptotically and locally exponentially converge to zero.

ARTICLE INFO

Article history:
Received 9 May 2012
Received in revised form
19 March 2013
Accepted 12 April 2013
Available online 3 May 2013

Keywords:
Bounded control
Global tracking
Mobile robots
One-step ahead backstepping method
Lyapunov's direct method

ABSTRACT

This paper presents a design of bounded controllers with a predetermined bound for global path tracking control of unicycle-type mobile robots at the torque level. A new one-step ahead backstepping method is first introduced. The heading angle and linear velocity of the robots are then considered as immediate controls to force the position of the robots to globally and asymptotically track its reference path. These immediate controls are designed based on the one-step ahead backstepping method to yield bounded control laws. Next, the one-step ahead backstepping method is applied again to design bounded control torques of the robots with a pre-specified bound. The proposed control design ensures global asymptotical and local exponential convergence of the position and orientation tracking errors to zero, and bounded torques driving the robots. Experimental results on a Khepera mobile robot verify the proposed control controller.

1. Introduction

The control of underactuated mechanical systems including wheeled mobile robots has received a lot of attention from the control and robotics communities due to their theoretical control design difficulties but a wide range of applications, see [1–4] and references therein for an overview and interesting introductory examples in this interesting area. Mobile robots have inherent difficulties in feedback control since the tangent linearization of the wheeled mobile robots' kinematic is uncontrollable. In fact, a direct application of Brockett's necessary condition [5] for feedback stabilization implies that the wheeled mobile robots cannot be stabilized by a stationary continuous state feedback although they are open loop controllable. Consequently, the classical smooth control theory cannot be applied.

The above limited application of the classical control theory to controlling wheeled mobile robots motivates researchers to seek nonclassical control design methods. These methods range from discontinuous to time-varying ones. Usually, the mobile robot's kinematic is considered, see for example [6–11]. Since the mobile robots do not have direct control over velocities, a static mapping implementation requires a high-gain control law and cannot achieve global results, see [12, pp. 239–245] for a discussion on general nonlinear systems. To overcome the problems caused by the static mapping implementation, the dynamic model was considered in the control design, see for example [13–17] using the backstepping technique [18] and feedback linearization [19].

Unfortunately, the backstepping technique [18] cannot guarantee bounded control torques with a predetermined bound, which drive the mobile robots' wheels. Moreover, all the wheeled mobile robots have bounded or saturated torques driving the wheels. Therefore, in the aforementioned control designs, which used the backstepping technique, one needs to apply one of the following two options. The first option is to saturate the designed torques. Saturation of the designed torques will deteriorate the performance of the controlled system or even will result in an unstable controlled system. The second option is to limit the initial conditions so that the designed torques are within the limits. This means that the designed control system can only operate locally. It is noted that in [20] a technique, which is an extension of the

E-mail addresses: duc@curtin.edu.au, duc@mech.uwa.edu.au.

0921-8890/$ – see front matter
http://dx.doi.org/10.1016/j.robot.2013.04.014

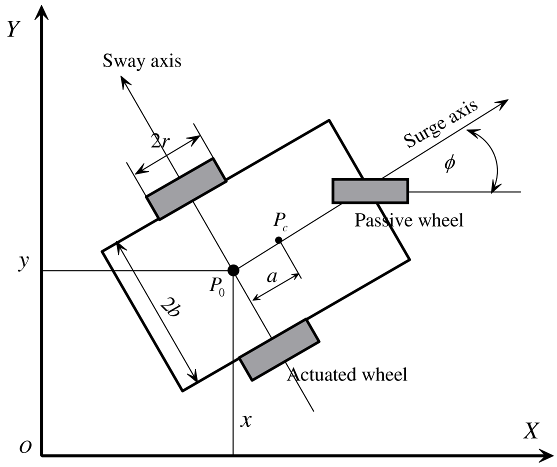

Fig. 1. Robot parameters.

backstepping technique in [18], was proposed to design a bounded controller for a certain class of nonlinear systems. However, this technique is not directly applied to a design of bounded torques with a pre-specified bound for the wheeled mobile robots under consideration.

The above discussions motivate contributions of this paper on designing bounded control torques with a specified bound for unicycle-type mobile robots. The paper introduces a new one-step ahead backstepping method. Using this method, the heading angle and linear velocity of the robots are used as (bounded) immediate controls to force the position of the robots to globally and asymptotically track its reference path. The one-step ahead backstepping method is again applied to design bounded control torques of the robots.

The rest of the paper is organized as follows. In Section 2, the mobile robot's equations of motion are presented. This section also includes a statement of control objectives. The one-step ahead backstepping method is introduced in Section 3. The control design is presented in Section 4. Section 5 gives experimental results on a Khepera mobile robot to verify the proposed control design. Proof of the main results is given in Appendix.

2. Problem statement

2.1. Mobile robot dynamics

We consider a unicycle-type mobile robot, which under the assumption of no wheel slips, has the following dynamics [21]:

$$\begin{cases} \dot{x} = v\cos(\phi) \\ \dot{y} = v\sin(\phi) \\ \dot{\phi} = w \end{cases},$$
$$\begin{bmatrix} \dot{v} \\ \dot{w} \end{bmatrix} = \bar{\boldsymbol{C}} \begin{bmatrix} w^2 \\ -vw \end{bmatrix} - \bar{\boldsymbol{D}} \begin{bmatrix} v \\ w \end{bmatrix} + \bar{\boldsymbol{B}}\boldsymbol{\tau}, \tag{1}$$

where (x, y) denotes the position (the coordinates of the middle point P_0 between the left and right driving wheels), ϕ denotes the heading angle of the robot coordinated in the earth-fixed frame OXY, see Fig. 1, v and w denote the linear and angular velocities of the robot, and $\boldsymbol{\tau} = [\tau_1\ \tau_2]^T$ with τ_1 and τ_2 being the control torques applied to the wheels of the robot. The positive definite matrices $\bar{\boldsymbol{C}}$ and $\bar{\boldsymbol{D}}$, and the invertible matrix $\bar{\boldsymbol{B}}$ are given by

$$\bar{\boldsymbol{C}} = \begin{bmatrix} \bar{c}_1 & 0 \\ 0 & \bar{c}_2 \end{bmatrix}, \qquad \bar{\boldsymbol{D}} = \begin{bmatrix} \bar{d}_{11} & \bar{d}_{12} \\ \bar{d}_{21} & \bar{d}_{22} \end{bmatrix}, \qquad \bar{\boldsymbol{B}} = \begin{bmatrix} \bar{b}_{11} & \bar{b}_{12} \\ \bar{b}_{21} & \bar{b}_{22} \end{bmatrix}, \tag{2}$$

where

$$\begin{aligned}
&\bar{c}_1 = \frac{bc}{m_{11}+m_{12}}, \qquad \bar{c}_2 = \frac{c}{b(m_{11}-m_{12})}, \\
&\bar{d}_{11} = \frac{d_{11}+d_{22}}{2(m_{11}+m_{12})}, \qquad \bar{d}_{12} = \frac{b(d_{11}-d_{22})}{2(m_{11}+m_{12})}, \\
&\bar{d}_{21} = \frac{d_{11}-d_{22}}{2b(m_{11}+m_{12})}, \qquad \bar{d}_{22} = \frac{d_{11}+d_{22}}{2(m_{11}+m_{12})}, \\
&\bar{b}_{11} = \frac{r}{2(m_{11}+m_{12})}, \qquad \bar{b}_{12} = \frac{r}{2(m_{11}+m_{12})}, \\
&\bar{b}_{21} = \frac{r}{2b(m_{11}-m_{12})}, \qquad \bar{b}_{22} = \frac{-r}{2b(m_{11}-m_{12})}, \\
&c = \frac{1}{2b}r^2 m_c a, \qquad m_{11} = \frac{1}{4b^2}r^2(mb^2+I)+I_w, \\
&m_{12} = \frac{1}{4b^2}r^2(mb^2-I), \\
&m = m_c + 2m_w, \qquad I = m_c a^2 + 2m_w b^2 + I_c + 2I_m.
\end{aligned} \tag{3}$$

In (3), m_c and m_w are the masses of the body and wheel with a motor; I_c, I_w, and I_m are the moments of inertia of the body about the vertical axis through P_c (center of mass), the wheel with the rotor of a motor about the wheel axis, and the wheel with the rotor of a motor about the wheel diameter, respectively; r, a, and b are defined in Fig. 1; the strictly positive constants d_{11} and d_{22} are the damping coefficients. It is noted that the robot dynamics (1) are a special form addressed in [22], see [23] for details.

2.2. Control objective

Control Objective 2.1. Assume that the reference path $\boldsymbol{\eta}_d(s) = [x_d(s)\ y_d(s)]^T$, with s being the path parameter, is non-singular, i.e., there exists a strictly positive constant ε_1 such that

$$x_d'^2(s) + y_d'^2(s) \geq \varepsilon_1, \tag{4}$$

where $x_d'(s) = \frac{\partial x_d}{\partial s}$ and $y_d'(s) = \frac{\partial y_d}{\partial s}$. The reference path linear velocity and linear acceleration are assumed to be bounded, i.e., there exist strictly positive constant ε_{21} and ε_{22} such that the following conditions hold:

$$\begin{aligned}
&\sqrt{x_d'^2(s(t)) + y_d'^2(s(t))}\,|\dot{s}(t)| \leq \varepsilon_{21}, \quad \forall t \geq 0, \\
&\left|\frac{d}{dt}\left(\sqrt{x_d'^2(s(t)) + y_d'^2(s(t))}\,\dot{s}(t)\right)\right| \leq \varepsilon_{22}, \quad \forall t \geq 0.
\end{aligned} \tag{5}$$

The positive constant ε_{21} satisfies the following condition

$$\varepsilon_{21} \leq \min(\bar{d}_{11}, \bar{d}_{22}) + \varrho_d, \tag{6}$$

where ϱ_d is a strictly positive constant. In addition, the path linear velocity is assumed to be persistently exciting, i.e., there exists a strictly positive constant ε_{23} such that for $t_2 > t_1 \geq 0$ the following conditions hold:

$$\lim_{t\to\infty}\left(\sqrt{x_d'^2(s(t)) + y_d'^2(s(t))}\dot{s}(t)\right)^2 \neq 0, \tag{7}$$

and

$$\int_{t_1}^{t_2}\left(\sqrt{x_d'^2(s(\tau)) + y_d'^2(s(\tau))}\dot{s}(\tau)\right)^2 d\tau \geq \varepsilon_{23}(t_2 - t_1). \tag{8}$$

The above definition of the reference path $\boldsymbol{\eta}_d$ gives

$$\begin{aligned}
&\dot{x}_d = \cos(\phi_d)v_d, \\
&\dot{y}_d = \sin(\phi_d)v_d,
\end{aligned} \tag{9}$$

where the reference linear velocity v_d is given by

$$v_d = \sqrt{x_d'^2 + y_d'^2}\,\dot{s}. \tag{10}$$

Under the above assumptions, design the control input vector $\boldsymbol{\tau}$ such that $\boldsymbol{\tau}$ is bounded with a specified bound and that the position vector $\boldsymbol{\eta}(t) = [x(t)\ y(t)]^T$ and the heading angle $\phi(t)$ of the robot globally asymptotically track their reference trajectories $\boldsymbol{\eta}_d(s(t))$ and $\phi_d(s(t))$, where

$$\phi_d(s(t)) = \arcsin\left(\frac{y_d'(s(t))}{\sqrt{x_d'^2(s(t)) + y_d'^2(s(t))}}\right). \tag{11}$$

Specifically for any initial conditions $\boldsymbol{\eta}(t_0) \in \mathbb{R}^2$, $\phi(t_0) \in \mathbb{R}$, and $(v(t_0), w(t_0)) \in \mathbb{R}^2$ at the initial time $t_0 \geq 0$ and under the no side slip nonholonomic constraint, design $\boldsymbol{\tau}$ such that

$$\begin{aligned} &\lim_{t\to\infty}(\boldsymbol{\eta}(t) - \boldsymbol{\eta}_d(s(t))) = 0, \qquad \lim_{t\to\infty}(\phi(t) - \phi_d(s(t))) = 0, \\ &\|\tau_1(t)\| \leq \tau_1^M, \qquad \|\tau_2(t)\| \leq \tau_2^M, \quad \forall t \geq t_0, \end{aligned} \tag{12}$$

where τ_1^M and τ_2^M are strictly positive constants.

Remark 2.1. The PE condition (5) implies that we are solving a path tracking control problem (not a stabilization problem) and that the reference path $\boldsymbol{\eta}_d$ can be a curve or a straight-line or a combination of both.

3. Preliminaries

In this section, we present a saturation function and the one-step ahead backstepping method, which will be used in the control design and stability analysis in the next section.

3.1. Smooth saturation function

This subsection defines the smooth saturation function that will be used in the control design later.

Definition 3.1. The function $\sigma(x)$ is said to be a smooth saturation function if it is smooth and possesses the properties:

(1) $\sigma(x) = 0$ if $x = 0$, $\quad \sigma(x)x > 0$ if $x \neq 0$,
(2) $\sigma(-x) = -\sigma(x)$, $(x-y)[\sigma(x) - \sigma(y)] \geq 0$,
(3) $|\sigma(x)| \leq 1$, $\quad \left|\frac{\sigma(x)}{x}\right| \leq 1$, $\quad \left|\frac{\mathrm{d}\sigma(x)}{\mathrm{d}x}\right| \leq 1$,

for all $(x, y) \in \mathbb{R}^2$. For the vector $\boldsymbol{x} = [x_1, \ldots, x_i, \ldots, x_n]^T$, the notation $\boldsymbol{\sigma}(\boldsymbol{x}) = [\sigma(x_1), \ldots, \sigma(x_i), \ldots, \sigma(x_n)]^T$ is used to denote the smooth saturation function vector of the vector $\boldsymbol{x}$.

Some functions satisfying the properties in Definition 3.1 include $\sigma(x) = \tanh(x)$ and $\sigma(x) = \frac{x}{\sqrt{1+x^2}}$.

3.2. One-step ahead backstepping method

This subsection presents the idea of the one-step ahead backstepping method through a simple example. This method will be used to design bounded controllers later. As such, consider the following second-order system:

$$\begin{aligned} \dot{x}_1 &= x_2, \\ \dot{x}_2 &= u \end{aligned} \tag{13}$$

where x_1 and x_2 are the states, and u is the control input. Let us address the problem of designing the control input u to globally and asymptotically stabilize (13) at the origin such that $|u(t)|$ is bounded by a predefined positive constant for all $t \geq t_0 \geq 0$, where t_0 is the initial time. The control design consists of two steps as follows:

Step 1. Define $x_{2e} = x_2 - \alpha_1$, where α_1 is the virtual control of x_2. Let us consider the Lyapunov function

$$V_1 = \int_0^{x_1} \sigma(s)ds, \tag{14}$$

where $\sigma(s)$ is a smooth saturation function defined in Definition 3.1. By differentiating both sides of (14), we choose the virtual control α_1 as

$$\alpha_1 = \frac{-k_1\sigma(x_1)}{\Delta_1(x_2)}, \tag{15}$$

where k_1 is a positive constant less than 1, and the function $\Delta_1(x_2)$ is chosen such that

$$\Delta_1(x_2) \geq 1, \qquad \left|\frac{\partial\alpha_1}{\partial x_2}\right| \leq k_1, \qquad \left|\frac{\partial\alpha_1}{\partial x_1}x_2\right| \leq k_1, \tag{16}$$

for all $(x_1, x_2) \in \mathbb{R}^2$. Using properties of the saturation function $\sigma(x_1)$ defined in Definition 3.1 and $\frac{\partial\alpha_1}{\partial x_2} = \frac{k_1\sigma(x_1)}{\Delta_1^2(x_2)}\frac{\mathrm{d}\Delta_1(x_2)}{\mathrm{d}x_2}$ and $\frac{\partial\alpha_1}{\partial x_1}x_2 = \frac{-k_1 x_2}{\Delta_1(x_2)}\frac{\mathrm{d}\sigma(x_1)}{\mathrm{d}x_1}$, the constraints on $\Delta_1(x_2)$ defined in (16) can be written as

$$\Delta_1(x_2) \geq 1, \qquad \left|\frac{\mathrm{d}\Delta_1(x_2)}{\mathrm{d}x_2}\right| \leq 1, \qquad \frac{|x_2|}{\Delta_1(x_2)} \leq 1. \tag{17}$$

A simple calculation shows that the functions $\Delta_1(x_2) = \sqrt{1+x_2^2}$ or $\Delta_1(x_2) = 1 + x_2^2$ satisfy the above constraints. Now substituting (15) and $x_{2e} = x_2 - \alpha_1$ into the derivative of V_1 results in

$$\dot{V}_1 = \frac{-k_1\sigma(x_1)^2}{\Delta_1(x_2)} + \sigma(x_1)x_{2e}. \tag{18}$$

Differentiating x_{2e} along the solutions of (13) and (15) gives

$$\dot{x}_{2e} = \left(1 - \frac{\partial\alpha_1}{\partial x_2}\right)u - \frac{\partial\alpha_1}{\partial x_1}x_2. \tag{19}$$

Step 2. Consider the Lyapunov function

$$V_2 = \gamma V_1 + \frac{1}{2}x_{2e}^2, \tag{20}$$

where γ is a positive constant. Differentiating both sides of (20) along the solutions of (18) and (19), and choosing the actual control u as

$$u = \left(1 - \frac{\partial\alpha_1}{\partial x_2}\right)^{-1}\left(-k_2\sigma(x_{2e}) - \gamma\sigma(x_1) + \frac{\partial\alpha_1}{\partial x_1}x_2\right) \tag{21}$$

result in

$$\dot{V}_2 = \frac{-k_1\gamma\sigma(x_1)^2}{\Delta_1(x_2)} - k_2\sigma(x_{2e})x_{2e}. \tag{22}$$

It is noted that since $\left|\frac{\partial\alpha_1}{\partial x_2}\right| \leq k_1$ for all $(x_1, x_2) \in \mathbb{R}^2$ and $k_1 < 1$, the control u given in (21) is well defined. Based on (14), (20) and (22), it is readily shown that the closed loop system consisting of (13) and (21) is forward complete and is globally asymptotically and locally exponential stable at the origin. Moreover, from (21) a calculation shows that

$$|u(t)| \leq \frac{k_1 + k_2 + \gamma}{1 - k_1}, \tag{23}$$

for all $t \geq t_0 \geq 0$. The above bound means that the magnitude of the control input u is bounded by an arbitrarily small positive constant for all $(x_1(t_0), x_2(t_0)) \in \mathbb{R}^2$ by choosing appropriate constants k_1, k_2, and γ.

Remark 3.1. (1) The main difference between the above control design and the standard backstepping method [18] is that the virtual control α_1 in (15) is a function of both x_1 and x_2. This is crucial to allow us to design the bounded control u in (21) with a predefined bound given in (23), see the term $\frac{\partial \alpha_1}{\partial x_1}x_2$. Indeed, if one set $\Delta_1(x_2) = 1$, the one-step ahead backstepping method becomes the standard backstepping technique in [18].
(2) There are several other methods (e.g., [24,25]) to design bounded control laws for a chain of integrators inspired by the work in [26]. However, it is difficult to apply these methods for designing global tracking controllers for the mobile robots in this paper.
(3) For simplicity, the above control design method has been presented for a second-order system (13). This method can be readily extended to a higher order system.

4. Control design

The control design consists of three steps. In the first step, the first two equations of (1) will be considered. Using the one-step ahead backstepping method introduced in Section 3.2, we will design the virtual controls of the heading angle ϕ and the linear velocity v to globally asymptotically stabilize the tracking error vector $\boldsymbol{\eta}(t) - \boldsymbol{\eta}_d(s(t))$ at the origin. In the second step, the third equation of (1) will be considered. Using the one-step ahead backstepping method the virtual control of the angular velocity w will be designed to globally asymptotically stabilize the error between the virtual control of the heading angle and the actual heading angle at the origin. In the last step, the last equation of (1) will be considered to design the actual control torque vector $\boldsymbol{\tau}$ to globally asymptotically stabilize the errors between the virtual controls of the linear and angular velocities and their actual values at the origin.

4.1. Step 1

In this step, we consider the first two equations of (1) to design the virtual controls of the heading angle ϕ and the linear velocity v to globally asymptotically and locally exponentially stabilize the tracking error vector $\boldsymbol{\eta}(t)-\boldsymbol{\eta}_d(s(t))$ at the origin. As such, we define

$$\begin{cases} x_e = x - x_d \\ y_e = y - y_d \end{cases}, \qquad \begin{cases} \phi_e = \phi - \alpha_\phi \\ v_e = v - \alpha_v \end{cases} \tag{24}$$

where α_ϕ and α_v are virtual controls of ϕ and v, respectively. Differentiating both sides of (24) along the solutions of the first two equations of (1) and (9) results in

$$\begin{aligned} \dot{x}_e &= \cos(\alpha_\phi)\alpha_v - \cos(\phi_d)v_d + \Theta_{11} + \Theta_{12}, \\ \dot{y}_e &= \sin(\alpha_\phi)\alpha_v - \sin(\phi_d)v_d + \Theta_{21} + \Theta_{22}, \end{aligned} \tag{25}$$

where

$$\begin{aligned} \Theta_{11} &= \left[\cos(\alpha_\phi)(\cos(\phi_e) - 1) - \sin(\alpha_\phi)\sin(\phi_e)\right]\alpha_v, \\ \Theta_{12} &= \cos(\phi)v_e, \\ \Theta_{21} &= \left[\sin(\alpha_\phi)(\cos(\phi_e) - 1) + \cos(\alpha_\phi)\sin(\phi_e)\right]\alpha_v, \\ \Theta_{22} &= \sin(\phi)v_e. \end{aligned} \tag{26}$$

To design the virtual controls α_v and α_ϕ, we consider the Lyapunov function candidate

$$V_1 = \int_0^{x_e} \sigma(\mu)d\mu + \int_0^{y_e} \sigma(\mu)d\mu, \tag{27}$$

whose derivative along the solutions of (25) is

$$\begin{aligned} \dot{V}_1 = {} & \sigma(x_e)\left(\cos(\alpha_\phi)\alpha_v - \cos(\phi_d)v_d + \Theta_{11} + \Theta_{12}\right) \\ & + \sigma(y_e)\left(\sin(\alpha_\phi)\alpha_v - \sin(\phi_d)v_d + \Theta_{21} + \Theta_{22}\right), \end{aligned} \tag{28}$$

which suggests that we use the one-step ahead backstepping method introduced in Section 3.2 to design the virtual controls α_v and α_ϕ such that

$$\begin{aligned} \cos(\alpha_\phi)\alpha_v - \cos(\phi_d)v_d &= -\frac{kv_d^2\sigma(x_e)}{\Delta(v,w)}, \\ \sin(\alpha_\phi)\alpha_v - \sin(\phi_d)v_d &= -\frac{kv_d^2\sigma(y_e)}{\Delta(v,w)}, \end{aligned} \tag{29}$$

where k is a positive constant to be chosen later, and the term $\Delta(v, w)$ is chosen as

$$\Delta(v,w) = \varrho_0 + 0.5(v^2 + w^2), \tag{30}$$

where ϱ_0 is a positive constant to be chosen later. The above choice of $\Delta(v, w)$ is not only motivated by the one-step backstepping method but also important for obtaining a bounded torque control vector $\boldsymbol{\tau}$ with a predetermined bound due to the Coriolis term $\bar{\boldsymbol{C}}[w^2 \;\; -vw]^T$ in (1), see Step 3. Moreover, to make the virtual control α_ϕ independent of the robot's linear and angular velocities v and w (due to the term $\Delta(v, w)$), we choose the path parameter update $\dot{s}$ as

$$\dot{s} = \frac{1}{\Delta(v,w)}\xi_d, \tag{31}$$

where ξ_d is referred to as the scaled path parameter update. The scaled path parameter update ξ_d specifies roughly how fast the robot should move on the path at the steady state. It is noted that if the path parameter update $\dot{s}$ was not chosen as in (31), there will be a *premature* control problem in the next step. Under the conditions (4) and (5), the scaled path parameter ξ_d needs to satisfy the following conditions:

$$|\dot{\xi}_d(t)| \le \varepsilon_{21}^*, \qquad |\ddot{\xi}_d(t)| \le \varepsilon_{22}^*, \quad \forall t \ge 0, \tag{32}$$

where ε_{21}^* and ε_{22}^* are strictly positive constants. The condition (32) means that the robot should move with bounded velocities and accelerations on the path at the steady state. The conditions (7) and (8) imply that

$$\lim_{t\to\infty} \xi_d^2(t) \ne 0 \tag{33}$$

and

$$\int_{t_1}^{t_2} \xi_d^2(\tau)d\tau \ge \varepsilon_{23}^*(t_2 - t_1), \quad \forall t_2 > t_1 \ge 0, \tag{34}$$

where ε_{23}^* is a strictly positive constant. The condition (34) implies that the path is persistently exciting. Solving (29) with the use of (31) and (10) for the virtual controls α_v and α_ϕ yields

$$\begin{aligned} \alpha_\phi = {} & \phi_d \\ & + \arctan\left(\frac{k\bar{v}_d(\sigma(x_e)\sin(\phi_d) - \sigma(y_e)\cos(\phi_d))}{-k\bar{v}_d(\sigma(x_e)\cos(\phi_d) + \sigma(y_e)\sin(\phi_d)) + 1}\right), \\ \alpha_v = {} & (-kv_d^2\Omega_1 + \cos(\phi_d)v_d)\cos(\alpha_\phi) \\ & + (-kv_d^2\Omega_2 + \sin(\phi_d)v_d)\sin(\alpha_\phi), \end{aligned} \tag{35}$$

where

$$\bar{v}_d = \sqrt{x_d'^2 + y_d'^2}\,\xi_d, \qquad \Omega_1 = \frac{\sigma(x_e)}{\Delta(v,w)}, \qquad \Omega_2 = \frac{\sigma(y_e)}{\Delta(v,w)}. \tag{36}$$

Since $|\sigma(x_e)| \le 1$ and $|\sigma(y_e)| \le 1$ for all $(x_e, y_e) \in \mathbb{R}^2$, we choose the positive constant k such that

$$k < \frac{1}{2}\sup_{t\in\mathbb{R}^+} |\bar{v}_d(t)|. \tag{37}$$

With this choice of k, it is seen that the virtual control α_ϕ given in (35) is well defined. It is seen from (35) with k satisfying the condition (37) that the virtual control α_ϕ is a smooth function of x_e, y_e, x'_d, y'_d and ξ_d, and the virtual control α_v is a smooth function of $x_e, y_e, x'_d, y'_d, \xi_d, v$, and w. Now, substituting (29) into (28) gives

$$\begin{aligned}\dot V_1 &= -\frac{kv_d^2\sigma^2(x_e)}{\Delta(v,w)} - \frac{kv_d^2\sigma^2(y_e)}{\Delta(v,w)} \\ &\quad + (\Theta_{11}+\Theta_{12})\sigma(x_e) + (\Theta_{21}+\Theta_{22})\sigma(y_e). \end{aligned} \tag{38}$$

This equation is to be used in the next step. It can be seen from this equation that if $\phi_e = 0$ and $v_e = 0$, i.e., the heading angle ϕ and the linear velocity v are considered as actual controls, the tracking errors x_e and y_e are globally asymptotically and locally exponentially stable at the origin because from (26) we have $\Theta_{11}|_{\phi_e=0} = \Theta_{21}|_{\phi_e=0} = 0$ and $\Theta_{12}|_{v_e=0} = \Theta_{22}|_{v_e=0} = 0$. To prepare for the next step, we calculate $\dot\phi_e$ and $\dot v_e$ by differentiating both sides of the second equation of (24) along the solutions of the first four equations of (1) to obtain

$$\begin{aligned}\dot\phi_e &= w - \frac{\partial\alpha_\phi}{\partial x_e}\Theta_{12} - \frac{\partial\alpha_\phi}{\partial y_e}\Theta_{22} + F_1, \\ \dot v_e &= \left(1-\frac{\partial\alpha_v}{\partial v}\right)\dot v - \frac{\partial\alpha_v}{\partial w}\dot w + F_2\end{aligned} \tag{39}$$

where

$$\begin{aligned} F_1 &= -\frac{\partial\alpha_\phi}{\partial x_e}\left(-\frac{kv_d^2\sigma(x_e)}{\Delta(v,w)} + \Theta_{11}\right) \\ &\quad - \frac{\partial\alpha_\phi}{\partial y_e}\left(-\frac{kv_d^2\sigma(y_e)}{\Delta(v,w)} + \Theta_{21}\right) - \frac{\partial\alpha_\phi}{\partial x'_d}x''_d\dot s \\ &\quad - \frac{\partial\alpha_\phi}{\partial y'_d}y''_d\dot s - \frac{\partial\alpha_\phi}{\partial\xi_d}\dot\xi_d, \\ F_2 &= -\frac{\partial\alpha_v}{\partial x_e}\left(-\frac{kv_d^2\sigma(x_e)}{\Delta(v,w)} + \Theta_{11}+\Theta_{12}\right) \\ &\quad - \frac{\partial\alpha_v}{\partial y_e}\left(-\frac{kv_d^2\sigma(y_e)}{\Delta(v,w)} + \Theta_{21}+\Theta_{22}\right) \\ &\quad - \frac{\partial\alpha_v}{\partial x'_d}x''_d\dot s - \frac{\partial\alpha_v}{\partial y'_d}y''_d\dot s - \frac{\partial\alpha_v}{\partial\xi_d}\dot\xi_d. \end{aligned} \tag{40}$$

4.2. Step 2

We define

$$w_e = w - \alpha_w, \tag{41}$$

where α_w is a virtual control of w. To design the virtual control α_w, we consider the Lyapunov function candidate

$$V_2 = \gamma_1 V_1 + \int_0^{\phi_e}\sigma(\mu)d\mu, \tag{42}$$

where γ_1 is a positive constant to be selected later. Differentiating both sides of (42) along the solutions of (38), (41), and the first equation of (39) gives

$$\begin{aligned}\dot V_2 &= -\frac{k\gamma_1 v_d^2\sigma^2(x_e)}{\Delta(v,w)} - \frac{k\gamma_1 v_d^2\sigma^2(y_e)}{\Delta(v,w)} \\ &\quad + \sigma(\phi_e)\Bigg[\alpha_w + F_1 + \gamma_1\sigma(x_e)\frac{\Theta_{11}}{\sigma(\phi_e)} \\ &\quad + \gamma_1\sigma(y_e)\frac{\Theta_{21}}{\sigma(\phi_e)}\Bigg] + \left(\gamma_1\sigma(x_e) - \sigma(\phi_e)\frac{\partial\alpha_\phi}{\partial x_e}\right)\Theta_{12} \\ &\quad + \left(\gamma_1\sigma(y_e) - \sigma(\phi_e)\frac{\partial\alpha_\phi}{\partial y_e}\right)\Theta_{22} + w_e\sigma(\phi_e). \end{aligned} \tag{43}$$

We choose the smooth saturation function $\sigma(\phi_e)$ such that the terms $\frac{\sin(\phi_e)}{\sigma(\phi_e)}$ and $\frac{1-\cos(\phi_e)}{\sigma(\phi_e)}$ and their first and second derivatives with respect to ϕ_e are bounded. There always exists such a function $\sigma(\phi_e)$. An example is $\sigma(\phi_e) = \tanh(\phi_e)$. With this choice of $\sigma(\phi_e)$, from the expressions of Θ_{11} and Θ_{21} in (26) we can see that the terms $\frac{\Theta_{11}}{\sigma(\phi_e)}$ and $\frac{\Theta_{21}}{\sigma(\phi_e)}$ in (43) are well defined and bounded. From (43), we use the one-step ahead backstepping method introduced in Section 3.2 to design the virtual control α_w as follows:

$$\alpha_w = -\frac{k_1\sigma(\phi_e)}{\Delta(v,w)} - F_1 - \gamma_1\sigma(x_e)\frac{\Theta_{11}}{\sigma(\phi_e)} - \gamma_1\sigma(y_e)\frac{\Theta_{21}}{\sigma(\phi_e)}, \tag{44}$$

where k_1 is a positive constant to be chosen later. It is seen from (44) that the virtual control α_w is a smooth function of $x_e, y_e, x'_d, x''_d, y'_d, y''_d, \xi_d, \dot\xi_d, \phi, v$ and w. Substituting (44) into (43) results in

$$\begin{aligned}\dot V_2 &= -\frac{k\gamma_1 v_d^2\sigma^2(x_e)}{\Delta(v,w)} - \frac{k\gamma_1 v_d^2\sigma^2(y_e)}{\Delta(v,w)} - \frac{k_1\sigma^2(\phi_e)}{\Delta(v,w)} \\ &\quad + \left(\gamma_1\sigma(x_e) - \sigma(\phi_e)\frac{\partial\alpha_\phi}{\partial x_e}\right)\Theta_{12} \\ &\quad + \left(\gamma_1\sigma(y_e) - \sigma(\phi_e)\frac{\partial\alpha_\phi}{\partial y_e}\right)\Theta_{22} + w_e\sigma(\phi_e). \end{aligned} \tag{45}$$

This equation is to be used in the next step. It can be seen from these equations that if $v_e = 0$ and $w_e = 0$, i.e., the linear and angular velocities are considered as actual controls, the tracking errors x_e, y_e, and ϕ_e are globally asymptotically and locally exponentially stable at the origin because from (26) we have $\Theta_{12}|_{v_e=0} = \Theta_{22}|_{v_e=0} = 0$.

To prepare for the next step, we calculate $\dot w_e$ by differentiating both sides of (41) with a note that α_w is a smooth function of $x_e, y_e, x'_d, y'_d, x''_d, y''_d, \xi_d, \dot\xi_d, \phi, v$ and w to obtain

$$\dot w_e = \left(1 - \frac{\partial\alpha_w}{\partial w}\right)\dot w - \frac{\partial\alpha_w}{\partial v}\dot v + F_3, \tag{46}$$

where

$$\begin{aligned} F_3 &= -\frac{\partial\alpha_w}{\partial x_e}\left(-\frac{kv_d^2\sigma(x_e)}{\Delta(v,w)} + \Theta_{11}+\Theta_{12}\right) \\ &\quad - \frac{\partial\alpha_w}{\partial y_e}\left(-\frac{kv_d^2\sigma(y_e)}{\Delta(v,w)} + \Theta_{21}+\Theta_{22}\right) \\ &\quad - \frac{\partial\alpha_w}{\partial x'_d}x''_d\dot s - \frac{\partial\alpha_w}{\partial y'_d}y''_d\dot s \\ &\quad - \frac{\partial\alpha_w}{\partial x''_d}x'''_d\dot s - \frac{\partial\alpha_w}{\partial y''_d}y'''_d\dot s \\ &\quad - \frac{\partial\alpha_w}{\partial\xi_d}\dot\xi_d - \frac{\partial\alpha_w}{\partial\dot\xi_d}\ddot\xi_d - \frac{\partial\alpha_w}{\partial\phi}w. \end{aligned} \tag{47}$$

Now substituting $\dot v$ and $\dot w$ from the last equation of (1) into the first equation of (39) and (46), and using $v = v_e + \alpha_v$ and $w = w_e + \alpha_w$ as defined in (24) and (41), we obtain:

$$\begin{aligned}\begin{bmatrix}\dot v_e \\ \dot w_e\end{bmatrix} &= \bar{\boldsymbol{C}}\begin{bmatrix} w_e^2 \\ -v_e w_e\end{bmatrix} - \bar{\bar{\boldsymbol{D}}}\begin{bmatrix} v_e \\ w_e\end{bmatrix} \\ &\quad + \bar{\boldsymbol{C}}\begin{bmatrix}\alpha_w^2 \\ -\alpha_v\alpha_w\end{bmatrix} - \boldsymbol{G}\bar{\boldsymbol{C}}\begin{bmatrix} w^2 \\ -vw\end{bmatrix} \\ &\quad - (\boldsymbol{I}_2 - \boldsymbol{G})\bar{\boldsymbol{D}}\begin{bmatrix}\alpha_v \\ \alpha_w\end{bmatrix} + \begin{bmatrix} F_2 \\ F_3\end{bmatrix} + (\boldsymbol{I}_2 - \boldsymbol{G})\bar{\boldsymbol{B}}\boldsymbol{\tau}, \end{aligned} \tag{48}$$

where

$$\bar{\bar{\boldsymbol{D}}} = (\boldsymbol{I}_2 - \boldsymbol{G})\bar{\boldsymbol{D}} - \bar{\boldsymbol{C}}\begin{bmatrix} 0 & 2\alpha_w \\ -\alpha_v & -\alpha_w \end{bmatrix},$$
$$\boldsymbol{G} = \begin{bmatrix} \frac{\partial \alpha_v}{\partial v} & \frac{\partial \alpha_v}{\partial w} \\ \frac{\partial \alpha_w}{\partial v} & \frac{\partial \alpha_w}{\partial w} \end{bmatrix} := \begin{bmatrix} g_{11} & g_{12} \\ g_{21} & g_{22} \end{bmatrix}, \tag{49}$$

with $\boldsymbol{I}_2$ being the 2 by 2 identity matrix. It is noted that $\det(\boldsymbol{I}_2 - \boldsymbol{G}) = \left(1 - \frac{\partial \alpha_v}{\partial v}\right)\left(1 - \frac{\partial \alpha_w}{\partial w}\right) - \frac{\partial \alpha_v}{\partial w}\frac{\partial \alpha_w}{\partial v} \geq 1 - (\chi_{11} + \chi_{22} + \chi_{11}\chi_{22} + \chi_{12}\chi_{21})$, where

$$\chi_{11} = \frac{6k\bar{v}_{dM}^2}{\varrho_0^4} + \frac{2\bar{v}_{dM}}{\varrho_0}, \qquad \chi_{12} = \frac{6k\bar{v}_{dM}^2}{\varrho_0^4} + \frac{2\bar{v}_{dM}}{\varrho_0},$$
$$\chi_{21} = \frac{k_1}{\varrho_0} + \frac{6k^2\bar{v}_{dM}^3}{\varrho_0^4} + \frac{2k\xi_d^2}{\varrho_0}(|x_d''| + |y_d''|), \tag{50}$$
$$\chi_{22} = \frac{k_1}{\varrho_0} + \frac{6k^2\bar{v}_{dM}^3}{\varrho_0^4} + \frac{2k\xi_d^2}{\varrho_0}(|x_d''| + |y_d''|),$$

with $\bar{v}_{dM} = \sup_{t\in\mathbb{R}^+} |\bar{v}_d(t)|$. Thus, we first choose the positive constants k, k_1, and ϱ_0 such that

$$1 - (\chi_{11} + \chi_{22} + \chi_{11}\chi_{22} + \chi_{12}\chi_{21}) > 0 \tag{51}$$

to make the matrix $(\boldsymbol{I}_2 - \boldsymbol{G})$ invertible. From (35) and (44) with F_1 given in (40), we have the bounds:

$$|\alpha_v| \leq \frac{2k\bar{v}_{dM}^2}{\varrho_0^3} + 2\bar{v}_{dM} := \alpha_{vM},$$
$$|\alpha_w| \leq \frac{2k\bar{v}_{dM}^3}{\varrho_0^4} + 12k\bar{v}_{dM}|\alpha_v| + 2k|\xi_d|(|x_d''| + |y_d''|) \tag{52}$$
$$+ k\sqrt{x_d'^2 + y_d'^2} \qquad |\dot{\xi}_d| := \alpha_{wM}.$$

We now derive the condition such that the matrix $\bar{\bar{\boldsymbol{D}}}$ is nonnegative definite. As such, expanding (49) results in

$$\bar{\bar{\boldsymbol{D}}} = \begin{bmatrix} (1 - g_{11})\bar{d}_{11} - g_{12}\bar{d}_{21} & (1 - g_{11})\bar{d}_{12} - g_{12}\bar{d}_{22} - 2\bar{c}_1\alpha_w \\ -g_{11}\bar{d}_{11} - (1 - g_{22})\bar{d}_{21} + \bar{c}_2\alpha_v & (1 - g_{22})\bar{d}_{22} - g_{21}\bar{d}_{12} + \bar{c}_2\alpha_w \end{bmatrix}$$
$$:= \begin{bmatrix} \bar{\bar{d}}_{11} & \bar{\bar{d}}_{12} \\ \bar{\bar{d}}_{21} & \bar{\bar{d}}_{22} \end{bmatrix}, \tag{53}$$

where $\bar{c}_1, \bar{c}_2, \bar{d}_{11}, \bar{d}_{12}, \bar{d}_{21}$ and $\bar{d}_{22}$ are defined in (3), and g_{11}, g_{12}, g_{21}, and g_{22} are defined in (49). Therefore the matrix $\bar{\bar{\boldsymbol{D}}}$ is nonnegative definite if the control gains k, k_1 and ϱ_0 such that

$$\bar{\bar{d}}_{11} \geq 0, \qquad (\bar{\bar{d}}_{11}\bar{\bar{d}}_{22} - \bar{\bar{d}}_{12}\bar{\bar{d}}_{21}) \geq 0. \tag{54}$$

Under the conditions (37), (32) and (6), there always exist k, k_1 and ϱ_0 such that the condition (54) holds.

4.3. Step 3

In this final step, we design the actual control vector $\boldsymbol{\tau}$ by considering (48). To design $\boldsymbol{\tau}$, we consider the following Lyapunov function candidate

$$V_3 = \gamma_2 V_2 + \frac{1}{2}[v_e \; w_e]\bar{\boldsymbol{C}}^{-1}\begin{bmatrix} v_e \\ w_e \end{bmatrix}, \tag{55}$$

where γ_2 is a positive constant to be chosen later. By differentiating both sides of (55) along the solutions of (48), we can design the control vector $\boldsymbol{\tau}$ as follows:

$$\boldsymbol{\tau} = \left((\boldsymbol{I}_2 - \boldsymbol{G})\bar{\boldsymbol{B}}\right)^{-1} \times \left(-\bar{\boldsymbol{C}}\gamma_2 \begin{bmatrix} \left(\gamma_1\sigma(x_e) - \sigma(\phi_e)\frac{\partial \alpha_\phi}{\partial x_e}\right)\cos(\phi) + \left(\gamma_1\sigma(y_e) - \sigma(\phi_e)\frac{\partial \alpha_\phi}{\partial y_e}\right)\sin(\phi) \\ \sigma(\phi_e) \end{bmatrix} - \begin{bmatrix} k_2\sigma(v_e) \\ k_3\sigma(w_e) \end{bmatrix} - \bar{\boldsymbol{C}}\begin{bmatrix} \alpha_w^2 \\ -\alpha_v\alpha_w \end{bmatrix} + \boldsymbol{G}\bar{\boldsymbol{C}}\begin{bmatrix} w^2 \\ -vw \end{bmatrix} + (\boldsymbol{I}_2 - \boldsymbol{G})\bar{\boldsymbol{D}}\begin{bmatrix} \alpha_v \\ \alpha_w \end{bmatrix} - \begin{bmatrix} F_2 \\ F_3 \end{bmatrix} \right), \tag{56}$$

where k_2 and k_3 are positive constants. Since for all $x_e \in \mathbb{R}$, $y_e \in \mathbb{R}$, $\phi \in \mathbb{R}$, $v \in \mathbb{R}$ and $w \in \mathbb{R}$, $\left\|\boldsymbol{G}[w^2 \; -vw]^T\right\|$, see (49) for the expression of $\boldsymbol{G}$, is bounded, and α_v and α_w are also bounded, see (52) for the bounds of α_v and α_w. From these bounds, we can calculate the bound of $|\tau_1|$ and $|\tau_2|$. This calculation is shown in Appendix A.3, i.e., there exist strictly positive constants τ_{1M} and τ_{2M} depending on only the reference trajectory and the control design parameters $\varepsilon_1, \varepsilon_{21}, \varepsilon_{22}, \varepsilon_{21}^*, \varepsilon_{22}^*, \gamma_1, \gamma_2, k, k_1, k_2, k_3$, and ϱ_0 such that

$$|\tau_1| \leq \tau_{1M}, \qquad |\tau_2| \leq \tau_{2M}, \tag{57}$$

for all $(x_e, y_e, \phi, v, w) \in \mathbb{R}^5$. The control vector $\boldsymbol{\tau}$ designed in (56) results in the derivative of V_3 as

$$\dot{V}_3 \leq -\frac{k\gamma_1\gamma_2 v_d^2\sigma^2(x_e)}{\Delta(v, w)} - \frac{k\gamma_1\gamma_2 v_d^2\sigma^2(y_e)}{\Delta(v, w)} - \frac{k_1\gamma_2\sigma^2(\phi_e)}{\Delta(v, w)} - [v_e \; w_e]\bar{\boldsymbol{C}}^{-1}\begin{bmatrix} k_2\sigma(v_e) \\ k_3\sigma(w_e) \end{bmatrix}, \tag{58}$$

where we have used the fact that under the condition (54) that the matrix $\bar{\bar{\boldsymbol{D}}}$ is positive definite. From (27), (42) and (55), we can see that V_3 is positive definite and radially unbounded, and its derivative given by (58) is negative definite. These properties will be used in stability analysis in Appendix.

From the control design above, we can write down the closed loop system by substituting (29) into (25), (44) into the first equation of (39), and (56) into (48) as follows:

$$\dot{x}_e = -\frac{kv_d^2\sigma(x_e)}{\Delta_1(v)} + \Theta_{11} + \Theta_{12},$$
$$\dot{y}_e = -\frac{kv_d^2\sigma(y_e)}{\Delta_1(v)} + \Theta_{21} + \Theta_{22},$$
$$\dot{\phi}_e = -\frac{k_1\sigma(\phi_e)}{\Delta(v, w)} - \gamma_1\sigma(x_e)\frac{\Theta_{11}}{\sigma(\phi_e)} - \gamma_1\sigma(y_e)\frac{\Theta_{21}}{\sigma(\phi_e)} - \frac{\partial \alpha_\phi}{\partial x_e}\Theta_{12} - \frac{\partial \alpha_\phi}{\partial y_e}\Theta_{22} + w_e, \tag{59}$$
$$\begin{bmatrix} \dot{v}_e \\ \dot{w}_e \end{bmatrix} = \bar{\boldsymbol{C}}\begin{bmatrix} w_e^2 \\ -v_e w_e \end{bmatrix} - \bar{\bar{\boldsymbol{D}}}\begin{bmatrix} v_e \\ w_e \end{bmatrix} - \begin{bmatrix} k_2\sigma(v_e) \\ k_3\sigma(w_e) \end{bmatrix} - \bar{\boldsymbol{C}}\begin{bmatrix} \gamma_1\gamma_2(\cos(\phi)\sigma(x_e) + \sin(\phi)\sigma(y_e)) \\ \gamma_2\sigma(\phi_e) \end{bmatrix}.$$

The control design has been completed. We summarize the results in the following theorem.

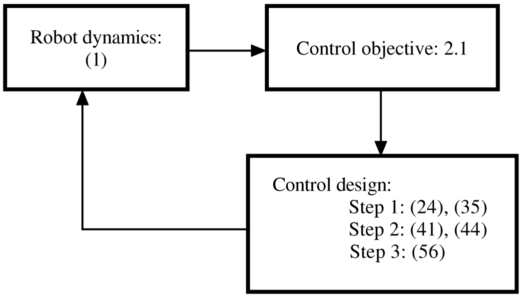

Fig. 2. Control design structure.

Fig. 3. The Khepera mobile robot.

Theorem 4.1. *Under the assumptions that the reference position trajectory $\boldsymbol{\eta}_d(t)$ satisfies the conditions (4) and (5), the control vector $\boldsymbol{\tau}$ given in (56) solves Control Objective 2.1 as long as the control gains $\gamma_1, \gamma_2, k, k_1, k_2, k_3$, and ϱ_0 are chosen such that the conditions (37), (51), (54) and (72) hold. In particular, the following hold for all initial conditions $\boldsymbol{\eta}(t_0) \in \mathbb{R}^2$, $\phi(t_0) \in \mathbb{R}$, and $(v(t_0), w(t_0)) \in \mathbb{R}^2$:*

(1) *The closed loop system (59) is forward complete.*
(2) *The tracking errors $\boldsymbol{\eta}(t) - \boldsymbol{\eta}_d(t)$ and $\phi(t) - \phi_d(t)$ are globally asymptotically stable at the origin, if the condition (7) or (33) holds. In addition, these tracking errors are locally exponentially stable at the origin, if the condition (8) or (34) holds.*
(3) *The control vector $\boldsymbol{\tau}$ is bounded. The bound can be pre-specified by (57) with τ_{1M} and τ_{2M} given in (72).*

Proof. See Appendix. The proposed control design is summarized in Fig. 2. □

Remark 4.1. If we set $\Delta = 1$, then the proposed control design becomes a known result in [16]. However, in this case the control torques τ_1 and τ_2 are no longer bounded with a predetermined bound.

5. Experimental results

This section presents experimental results on a small-size Khepera mobile robot (diameter of 0.07 m, height of 0.03 m, and weight of 0.08 kg), see Fig. 3, to verify the proposed controller designed in the previous section. Developed for educational and research purposes by the K-Team (see the URL http://www.k-team.com for more information), the Khepera mobile robot has several proximity sensors (not used in the experiments) and can work in a semi-autonomous (server–client) or completely autonomous mode. The Khepera mobile robot uses two DC motor driven wheels. The DC motors are connected to the wheels through a 25:1 reduction gear box. Two incremental encoders are placed on the motor axes. The resolution of the encoder is 24 pulses per revolution of motor axis. This corresponds to $24 \times 25 = 600$ pulses per revolution of the wheels or 12 pulses per millimeter of wheel displacement. The algorithm to estimate the velocity from the encoder output is implemented on the robot. Communication between the Khepera mobile robot and a host computer is performed via a RS-232 serial port. We use the PCMCIA-232/4 card from National Instruments™ for RS-232 communication between the robot and the host computer.

The physical parameters of the robot are: $b = 0.03$ m, $a = 0$ m, $r = 0.01$ m, $m_c = 0.07$ kg, $m_w = 0.005$ kg, $I_c = 0.04$ kg m^2, $I_w = 2.5 \times 10^{-5}$ kg m^2, $I_m = 1.25 \times 10^{-5}$ kg m^2, $d_{11} = d_{22} = 0.01$ kg/s. A program is written in LabWindows™/CVI (a C/C++ programming language with an easy development of user interface and hardware interface), a product of National Instruments™, to implement the control algorithm developed in this paper. In the experiment, an eight-shaped reference path is chosen as

$$\boldsymbol{\eta}_d(s) = \begin{bmatrix} 1.4\sin(s/20) \\ 0.5\sin(s/10) \end{bmatrix}. \tag{60}$$

The scaled path parameter ξ_d is chosen as $\xi_d = 0.5$. The initial conditions are chosen as

$$\boldsymbol{\eta}(0) = \begin{bmatrix} 0\text{ m} \\ -0.14\text{ m} \end{bmatrix}, \qquad \phi(0) = \frac{\pi}{6}\text{ rad}, \qquad \begin{bmatrix} v(0) \\ w(0) \end{bmatrix} = \begin{bmatrix} 0\text{ m/s} \\ 0\text{ rad/s} \end{bmatrix}. \tag{61}$$

The upper-bounds τ_{1M} and τ_{2M} of the control torques τ_1 and τ_2 are $\tau_{1M} = \tau_{2M} = 0.25$ N m. We experimentally determine the maximum torques provided by the Khepera mobile robot of about 0.5 Nm. The smooth saturation function $\sigma(\bullet)$ is chosen as $\sigma(\bullet) = \tanh(\bullet)$. With the above reference path and the upper-bounds of the control torques, the control gains are chosen as $\gamma_1 = \gamma_2 = 1$, $k = 0.5$, $k_1 = 0.5$, $k_2 = k_3 = 1$, and $\varrho_0 = 5$ so that they satisfy all the conditions (4), (5) and (33), and (33), and (72). The sampling rate is 10 Hz.

Experimental results are presented in Figs. 4 and 5. Fig. 4 is the main user interface panel of the program. It provides the robot (red dot) and reference (solid blue line) trajectories. The user can see the real time value of the position and heading of the robot, and log the data for postprocessing. The position tracking errors x_e and y_e are plotted in Fig. 5(a). The heading angle tracking error ϕ_e is plotted in Fig. 5(b). The robot velocities v and w are plotted in Fig. 5(c) and Fig. 5(d). Fig. 5(e) plots the control torques τ_1 and τ_2. It is seen from these figures that the proposed controller forces the robot to track the path very well and that the control torques τ_1 and τ_2 are both bounded by their preset maximum values τ_{1M} and τ_{2M}. The position and heading tracking errors do not actually converge to zero due to the noise and an inaccurate calculation of the robot's parameters. However, this shows certain robustness of the proposed control design. The above robustness properties are due to global asymptotic and local exponential stability of the tracking errors at the origin. Indeed, if the uncertainties in the robot's parameters and noise are larger, a modification of the proposed control design to a robust adaptive version using the control design proposed in this paper and the techniques in [10,27] should be addressed to achieve a better performance.

6. Conclusions

This paper addressed the problem of designing global path tracking controllers for the mobile robots. Appropriately chosen control design parameters and settings guarantee that the control torque $\boldsymbol{\tau}$ obtained by the proposed control algorithm does not exceed a predefined upper bound. This was achieved by the development of the novel one-step ahead backstepping method in

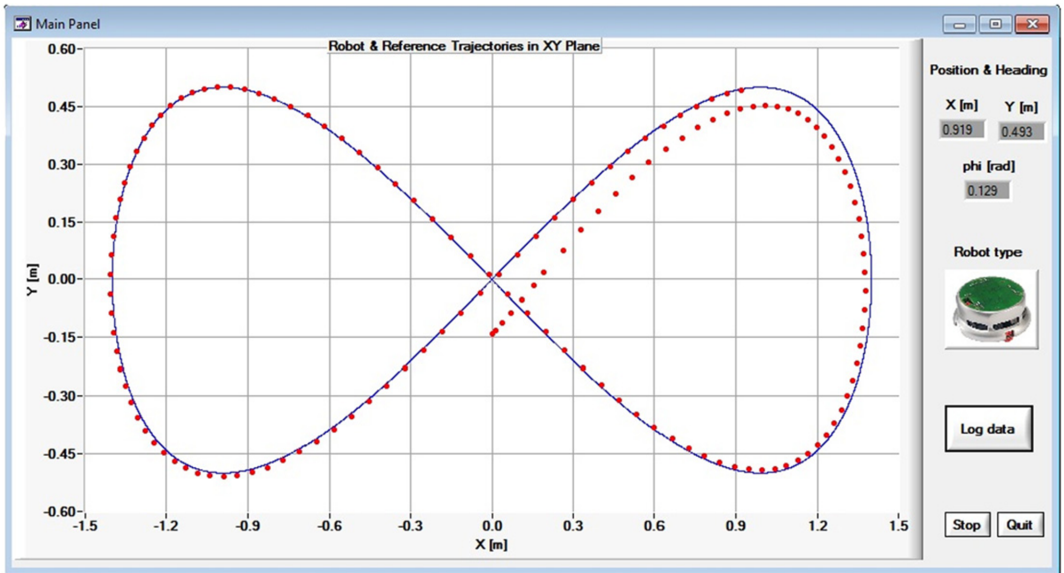

Fig. 4. Experimental results: robot (red dot) and reference (solid blue line) trajectories.

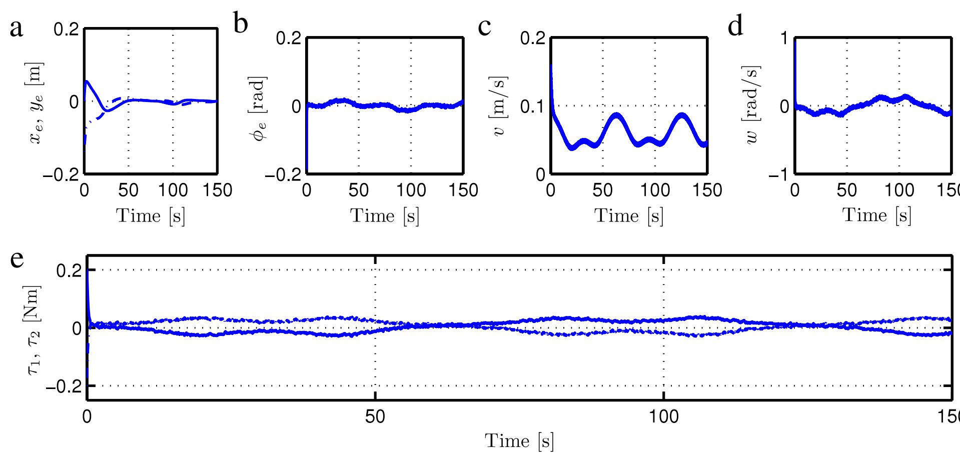

Fig. 5. Experimental results: (a) position tracking errors; (b) heading tracking error; (c) robot linear velocity; (d) robot angular velocity; (e) control torques.

Section 3.2 and the control design procedure in Section 4. The one-step backstepping method and the above control design procedure can be applied to the design of a bounded controller with a predefined upper bound for other systems modeled by a chain of integrators or linear systems perturbed by certain nonlinearities. The future work is to extend the proposed control design in this paper and combine with the control design techniques in [28] to design bounded controllers at the torque/force level for global path tracking control of underactuated surface ships.

Appendix. Proof of Theorem 4.1

To prove Theorem 4.1, we first show that the closed loop system (59) is forward complete. Second, we prove that the robot's position $\boldsymbol{\eta}(t)$ and the robot's heading angle $\phi(t)$ globally asymptotically and locally exponentially track their reference trajectories $\boldsymbol{\eta}_d(t)$ and $\phi_d(t)$. Finally, we show that the torque control vector $\boldsymbol{\tau}$ is bounded.

A.1. Proof of forward completeness of the closed loop system

To prove that the closed loop system (59) is forward complete, we substitute V_1 defined in (27) into V_2 defined in (42) and then into V_3 defined in (55) to obtain

$$V_3 = \gamma_1\gamma_2\left(\int_0^{x_e}\sigma(\mu)d\mu + \int_0^{y_e}\sigma(\mu)d\mu\right) + \gamma_2\int_0^{\phi_e}\sigma(\mu)d\mu + \frac{1}{2}[v_e\ w_e]\overline{\boldsymbol{C}}^{-1}\begin{bmatrix} v_e \\ w_e \end{bmatrix}, \tag{62}$$

which is positive definite and radially unbounded in x_e, y_e, ϕ_e, v_e, and w_e because γ_1 and γ_2 are positive constants, and the matrix $\overline{\boldsymbol{C}}$ is positive definite. On the other hand, it is seen from (58) that $\dot{V}_3 \leq 0$ for all $x_e \in \mathbb{R}, y_e \in \mathbb{R}, \phi_e \in \mathbb{R}, v_e \in \mathbb{R}$, and $w_e \in \mathbb{R}$. Therefore $V_3(t) \leq V_3(t_0)$ for all $t \geq t_0 \geq 0$, which implies that $x_e(t), y_e(t), \phi_e(t), v_e(t)$, and $w_e(t)$ are bounded for all $t \geq t_0 \geq 0$. Existence of $x_e(t), y_e(t), \phi_e(t), v_e(t)$, and $w_e(t)$ for all $t \geq t_0 \geq 0$ implies that the closed loop system (59) is forward complete. Moreover, $V_3(t) \leq V_3(t_0)$ implies that $v(t)$ and $w(t)$ are bounded, i.e., there exist nonnegative constants v_0 and w_0 such that

$$|v(t)| \leq v_0, \qquad |w(t)| \leq w_0, \tag{63}$$

for all $t \geq t_0 \geq 0$, since we have already proved that $x_e(t)$, $y_e(t)$, $\phi_e(t)$, $v_e(t)$, and $w_e(t)$ are bounded, and $\alpha_v(t)$ and $\alpha_w(t)$ are also bounded for all $t \geq t_0 \geq 0$, see (52).

A.2. Proof of convergence of $\boldsymbol{\eta}(t)$ and $\phi(t)$

To prove that the robot's position $\boldsymbol{\eta}(t)$ and the robot's heading angle $\phi(t)$ globally asymptotically and locally exponentially track their reference trajectories $\boldsymbol{\eta}_d(t)$ and $\phi_d(t)$, it is sufficient to prove that $x_e(t), y_e(t), \phi_e(t), v_e(t)$, and $w_e(t)$ globally asymptotically and locally exponentially converge to zero. As such, from (58) we have

$$\begin{aligned}\dot{V}_3 \le & -\frac{k\gamma_1\gamma_2\bar{v}_d^2\sigma^2(x_e)}{\Delta^3(v_0,w_0)}-\frac{k\gamma_1\gamma_2\bar{v}_d^2\sigma^2(y_e)}{\Delta^3(v_0,w_0)}\\ & -\frac{k_1\gamma_2\sigma^2(\phi_e)}{\Delta(v_0,w_0)}-[v_e\ w_e]\bar{\boldsymbol{C}}^{-1}\begin{bmatrix}k_2\sigma(v_e)\\ k_3\sigma(w_e)\end{bmatrix},\end{aligned}\tag{64}$$

where we have used (63), and $\Delta(v_0,w_0)=\Delta(v,w)|_{v=v_0,w=w_0}$. Now, applying Theorem 4.4 in [19] to (64) results in

$$\begin{aligned}\lim_{t\to\infty}\Bigg(&\frac{k\gamma_1\gamma_2\bar{v}_d^2(t)\sigma^2(x_e(t))}{\Delta^3(v_0,w_0)}+\frac{k\gamma_1\gamma_2\bar{v}_d^2(t)\sigma^2(y_e(t))}{\Delta^3(v_0,w_0)}\\ &+\frac{k_1\gamma_2\sigma^2(\phi_e(t))}{\Delta(v_0,w_0)}+[v_e\ w_e]\bar{\boldsymbol{C}}^{-1}\begin{bmatrix}k_2\sigma(v_e(t))\\ k_3\sigma(w_e(t))\end{bmatrix}\Bigg)=0.\end{aligned}\tag{65}$$

Under the condition (7) or (33), we have $\lim_{t\to\infty}\bar{v}_d^2(t)\neq 0$. Therefore, the limit (65) implies that

$$\lim_{t\to\infty}(x_e(t),y_e(t),\phi_e(t),v_e(t),w_e(t))=0,\tag{66}$$

where we have used the definition of the smooth saturation function $\sigma(\bullet)$ in Definition 3.1, and the fact that we have already proved $x_e(t), y_e(t), \phi_e(t), v_e(t)$, and $w_e(t)$ are bounded. The limits in (66) and the fact that V_3 is positive definite and radially unbounded in x_e, y_e, ϕ_e, v_e, and w_e mean that $x_e(t), y_e(t), \phi_e(t), v_e(t)$, and $w_e(t)$ globally asymptotically converge to zero.

We now show local exponential convergence of $x_e(t), y_e(t), \phi_e(t), v_e(t)$, and $w_e(t)$ to zero. Since we have proved that $x_e(t), y_e(t), \phi_e(t), v_e(t)$, and $w_e(t)$ globally asymptotically converge to zero, there exists a time T such that $x_e(t), y_e(t), \phi_e(t), v_e(t)$, and $w_e(t)$ are sufficiently small in their magnitudes for all $t\ge T\ge t_0\ge 0$. Therefore for all $t\ge T$, we can write (62) and (64) as

$$\begin{aligned}&\ell_m\|\boldsymbol{X}_e\|^2\le V_3\le\ell_M\|\boldsymbol{X}_e\|^2,\\ &\dot{V}_3\le -a_0(t)\|\boldsymbol{X}_e\|^2\le-\frac{a_0(t)}{\ell_M}V_3,\end{aligned}\tag{67}$$

for all $t\ge T\ge t_0\ge 0$, where

$$\begin{aligned}&\boldsymbol{X}_e=[x_e\ y_e\ \phi_e\ v_e\ w_e]^T,\\ &a_0(t)=\min\left(\frac{k\gamma_1\gamma_2\bar{v}_d^2(t)}{\Delta_0^3},\frac{k_1\gamma_2}{\Delta_0},\frac{1}{\bar{c}_1},\frac{1}{\bar{c}_2}\right),\\ &\ell_M=\frac{1}{2}\max\left(\gamma_1\gamma_2,\gamma_2,\frac{1}{\bar{c}_1},\frac{1}{\bar{c}_2}\right),\\ &\ell_m=\frac{1}{2}\min\left(\gamma_1\gamma_2,\gamma_2,\frac{1}{\bar{c}_1},\frac{1}{\bar{c}_2}\right),\end{aligned}\tag{68}$$

with Δ_0 being a positive constant (depending on the initial conditions) such that $\Delta_0\ge\Delta(v_0,w_0)$. Solving (67) and using $\int_T^t\bar{v}_d^2(\tau)d\tau\ge\varepsilon_1\varepsilon_{23}^*(t-T)$, see the conditions (4) and (7) or (34), yield

$$\begin{aligned}V_3 &\le V_3(T)e^{-\frac{1}{\ell_M}\int_T^t a_0(\tau)\mathrm{d}\tau}\Rightarrow V_3\\ &\le V_3(T)e^{-a_0^*(t-T)}\Rightarrow\|\boldsymbol{X}_e(t)\|\le\frac{\ell_M}{\ell_m}\|\boldsymbol{X}_e(t_0)\|e^{-\frac{a_0^*}{2}(t-T)},\end{aligned}\tag{69}$$

where $a_0^*=\frac{1}{\ell_M}\min\left(\frac{k\gamma_1\gamma_2\varepsilon_1\varepsilon_{23}^*}{\Delta_0^3},\frac{k_1\gamma_2}{\Delta_0},\frac{1}{\bar{c}_1},\frac{1}{\bar{c}_2}\right)$. Hence, we have local exponential convergence of $\boldsymbol{X}_e(t)$ to zero.

A.3. Bound of control torques τ_1 and τ_2

To calculate the bound of τ_1 and τ_2, we use the conditions (4), (5), (32), (37) with a note that $\Delta(v,w)$ is defined in (30). As such, we first calculate bounds of the following immediate terms:

$$\begin{aligned}
&\left|\frac{\partial\alpha_\phi}{\partial x_e}\right|\le\frac{k\bar{v}_{dM}}{1-k\bar{v}_{dM}}+\frac{2(k\bar{v}_{dM})^2}{(1-k\bar{v}_{dM})^2},\\
&\left|\frac{\partial\alpha_\phi}{\partial y_e}\right|\le\frac{k\bar{v}_{dM}}{1-k\bar{v}_{dM}}+\frac{2(k\bar{v}_{dM})^2}{(1-k\bar{v}_{dM})^2},\\
&\left|\frac{\partial\alpha_\phi}{\partial\bar{v}_d}\right|\le\frac{2k}{1-k\bar{v}_{dM}}+\frac{2k^2\bar{v}_{dM}}{(1-k\bar{v}_{dM})^2},\\
&\left|\frac{\partial^2\alpha_\phi}{\partial x_e^2}\right|\le 3\frac{k\bar{v}_{dM}(1+2k\bar{v}_{dM})+2(k\bar{v}_{dM})^2}{(1-k\bar{v}_{dM})^2},\\
&\left|\frac{\partial^2\alpha_\phi}{\partial y_e^2}\right|\le 3\frac{k\bar{v}_{dM}(1+2k\bar{v}_{dM})+2(k\bar{v}_{dM})^2}{(1-k\bar{v}_{dM})^2},\\
&\left|\frac{\partial^2\alpha_\phi}{\partial x_e\partial y_e}\right|\le 3\frac{k\bar{v}_{dM}(1+2k\bar{v}_{dM})+2(k\bar{v}_{dM})^2}{(1-k\bar{v}_{dM})^2},\\
&\left|\frac{\partial\alpha_\phi}{\partial\phi_d}\right|\le 1+\frac{2k\bar{v}_{dM}}{1-k\bar{v}_{dM}}+\frac{2k(\bar{v}_{dM})^2}{(1-k\bar{v}_{dM})^2},\\
&|\dot{\bar{v}}_d|\le\sqrt{x_{dM}'^2+y_{dM}'^2}\epsilon_{21}^*+\frac{x_{dM}'x_{dM}''+y_{dM}'y_{dM}''}{(x_{dm}'^2+y_{dm}'^2)^{3/2}}\xi_{dM}^2,\\
&|\dot{\phi}_d|\le\frac{x_{dM}'y_{dM}''+x_{dM}''y_{dM}'}{x_{dm}'^2+y_{dm}'^2}\xi_{dM},\\
&\left|\frac{\partial\alpha_w}{\partial x_e}\right|\le\left|\frac{\partial\alpha_\phi}{\partial x_e}\right|\left(\frac{kv_{dM}^2}{\varrho_0}+3\alpha_{vM}\left|\frac{\partial\alpha_\phi}{\partial x_e}\right|\right)\\
&\qquad+\left|\frac{\partial^2\alpha_\phi}{\partial x_e^2}\right|\left(\frac{kv_{dM}^2}{\varrho_0}+3\alpha_{vM}\right)\\
&\qquad+3\alpha_{vM}\left|\frac{\partial\alpha_\phi}{\partial y_e}\right|\left|\frac{\partial\alpha_\phi}{\partial x_e}\right|\\
&\qquad+\left|\frac{\partial^2\alpha_\phi}{\partial x_e\partial y_e}\right|\left(\frac{kv_{dM}^2}{\varrho_0}+3\alpha_{vM}\right)\\
&\qquad+\left|\frac{\partial\alpha_\phi}{\partial\bar{v}_d}\right||\dot{\bar{v}}_d|+\left|\frac{\partial\alpha_\phi}{\partial\phi_d}\right||\dot{\phi}_d|\\
&\qquad+3\gamma_1\alpha_{vM}+2\gamma_1 3\alpha_{vM}\left|\frac{\partial\alpha_\phi}{\partial x_e}\right|,\\
&\left|\frac{\partial\alpha_w}{\partial y_e}\right|\le\left|\frac{\partial\alpha_\phi}{\partial y_e}\right|\left(\frac{kv_{dM}^2}{\varrho_0}+3\alpha_{vM}\left|\frac{\partial\alpha_\phi}{\partial y_e}\right|\right)\\
&\qquad+\left|\frac{\partial^2\alpha_\phi}{\partial y_e^2}\right|\left(\frac{kv_{dM}^2}{\varrho_0}+3\alpha_{vM}\right)\\
&\qquad+3\alpha_{vM}\left|\frac{\partial\alpha_\phi}{\partial y_e}\right|\left|\frac{\partial\alpha_\phi}{\partial x_e}\right|\\
&\qquad+\left|\frac{\partial^2\alpha_\phi}{\partial x_e\partial y_e}\right|\left(\frac{kv_{dM}^2}{\varrho_0}+3\alpha_{vM}\right)\\
&\qquad+\left|\frac{\partial\alpha_\phi}{\partial\bar{v}_d}\right||\dot{\bar{v}}_d|+\left|\frac{\partial\alpha_\phi}{\partial\phi_d}\right||\dot{\phi}_d|\\
&\qquad+3\gamma_1\alpha_{vM}+2\gamma_1 3\alpha_{vM}\left|\frac{\partial\alpha_\phi}{\partial y_e}\right|,
\end{aligned}\tag{70}$$

for all $x_e\in\mathbb{R}, y_e\in\mathbb{R}, \phi\in\mathbb{R}, v\in\mathbb{R}$ and $w\in\mathbb{R}$, where the notations $\bullet_M$ and $\bullet_m$ denote the supremum and infimum values of $|\bullet(t)|$, respectively, with $t\in\mathbb{R}^+$, and α_{vM} is defined in (52). We can then use the calculated bounds in (70) to calculate bounds of

F_2 and F_3 defined in (40) and (47), respectively, as follows:

$$\begin{aligned}
|F_2| \leq{}& \left(\frac{4kv_{dM}}{\varrho_0} + \frac{1+2k\bar{v}_{dM}}{1-2k\bar{v}_{dM}}\right)\left(\sqrt{x'^2_{dM}+y'^2_{dM}}\,\varepsilon^*_{21} + \frac{x'_{dM}x''_{dM}+y'_{dM}y''_{dM}}{(x'^2_{dm}+y'^2_{dm})^{3/2}}\xi_{dM}\right) \\
&+ 2kv^2_{dM}\left(\frac{kv^2_{dM}}{\varrho_0} + 3\alpha_{vM} + \frac{1}{2\varrho_0}\right) + 2v_{dM}\frac{x'_{dM}y''_{dM}+x''_{dM}y'_{dM}}{x'^2_{dm}+y'^2_{dm}}\xi_{dM}, \\
|F_3| \leq{}& \left(\left|\frac{\partial\alpha_w}{\partial x_e}\right| + \left|\frac{\partial\alpha_w}{\partial y_e}\right|\right)\left(\frac{kv^2_{dM}}{\varrho_0} + 3\alpha_{vM} + \frac{1}{2\varrho_0}\right) \\
&+ \left(\frac{4kv_{dM}}{\varrho_0} + \frac{1+2k\bar{v}_{dM}}{1-2k\bar{v}_{dM}}\right)\Bigg(\sqrt{x'^2_{dM}+y'^2_{dM}}\,\varepsilon^*_{21} \\
&+ \frac{(x''^2_{dM}+x'_{dM}x'''_{dM}+y''^2_{dM}+y'_{dM}y'''_{dM})(x'^2_{dM}+y'^2_{dM}) + 1.5(x'_{dM}x''_{dM}+y'_{dM}y''_{dM})}{(x'^2_{dm}+y'^2_{dm})^{5/2}}\varepsilon^*_{22}\Bigg) \\
&+ k_1 + 2\alpha_{vM}\left|\frac{\partial\alpha_\phi}{\partial x_e}\right|,
\end{aligned} \tag{71}$$

where the bound of $\left|\frac{\partial\alpha_w}{\partial x_e}\right|$, $\left|\frac{\partial\alpha_w}{\partial y_e}\right|$, and $\left|\frac{\partial\alpha_\phi}{\partial x_e}\right|$ are given in (70). Now using (50) and (70), (71), we calculate the bound of τ_1 and τ_2 from (56) as follows:

$$\begin{aligned}
|\tau_1| &\leq \frac{(\chi_{21}\bar{b}_{12} + (1+\chi_{22})\bar{b}_{22})H_1 + (1+\chi_{11}\bar{b}_{12} + \chi_{12}\bar{b}_{22})H_2}{H_3} \\
&:= \tau_{1M}, \\
|\tau_2| &\leq \frac{(\chi_{21}\bar{b}_{11} + (1+\chi_{22})\bar{b}_{21})H_1 + (1+\chi_{11}\bar{b}_{11} + \chi_{12}\bar{b}_{12})H_2}{H_3} \\
&:= \tau_{2M},
\end{aligned} \tag{72}$$

for all $x_e \in \mathbb{R}$, $y_e \in \mathbb{R}$, $\phi \in \mathbb{R}$, $v \in \mathbb{R}$ and $w \in \mathbb{R}$, where

$$\begin{aligned}
H_1 &= k_2 + 2\gamma_2\bar{c}_1(\gamma_1 + kv_{dM}) + \bar{c}_1\alpha^2_{wM} \\
&\quad + \bar{c}_1\chi_{11} + \bar{c}_2\chi_{22} + ((1+\chi_{11})\bar{d}_{11} + \chi_{22}\bar{d}_{21})\alpha_{vM} \\
&\quad + ((1+\chi_{11})\bar{d}_{12} + \chi_{12}\bar{d}_{22})\alpha_{wM} + |F_2|, \\
H_2 &= k_3 + 2\gamma_2\bar{c}_2 + \bar{c}_2\alpha_{vM}\alpha_{wM} + ((1+\chi_{22})\bar{d}_{21} \\
&\quad + \chi_{21}\bar{d}_{11})\alpha_{vM} + ((1+\chi_{22})\bar{d}_{22} + \chi_{21}\bar{d}_{12})\alpha_{wM} + |F_3|, \\
H_3 &= ((1-\chi_{11})\bar{b}_{11} - \chi_{12}\bar{b}_{21})((1-\chi_{22})\bar{b}_{22} \\
&\quad - \chi_{21}\bar{b}_{12})((1+\chi_{11})\bar{b}_{12} + \chi_{12}\bar{b}_{22})(\chi_{21}\bar{b}_{11} \\
&\quad + (1+\chi_{22})\bar{b}_{21}).
\end{aligned} \tag{73}$$

It is seen from (50) and (70), (71), (73) that the bounds τ_{1M} of τ_1 and τ_{2M} of τ_2 defined in (72) depend on ε_1, ε_{21}, ε_{22}, ε^*_{21}, ε^*_{22}, γ_1, γ_2, k, k_1, k_2, k_3, and ϱ_0, i.e., the bound of the control torques τ_1 and τ_2 can be predetermined. □

References

[1] R. Murray, S. Sastry, Nonholonomic motion planning: steering using sinusoids, IEEE Transactions on Automatic Control 38 (5) (1993) 700–716.
[2] I. Kolmanovsky, N.H. McClamroch, Developments in nonholonomic control problems, IEEE Control Systems Magazine 6 (1995) 20–36.
[3] B. dAndrea Novel, G. Bastin, G. Campion, Control of nonholonomic wheeled mobile robots by state feedback linearization, International Journal of Robotics Research 14 (6) (1995) 543–559.
[4] A.M. Bloch, S. Drakunov, Stabilization and tracking in the nonholonomic integrator via sliding mode, Systems and Control Letters 29 (2) (1996) 91–99.
[5] R.W. Brockett, Asymptotic stability and feedback stabilization, in: R.W. Brockett, R.S. Millman, H.J. Sussmann (Eds.), Differential Geometric Control Theory, Birkhauser, Boston, 1983, pp. 181–191.
[6] C.d.W. Canudas, B. Siciliano, G. Bastin, Theory of Robot Control, Springer, London, 1996.
[7] A. Astolfi, Discontinuous control of the Brockett integrator, European Journal of Control 4 (1) (1998) 49–63.
[8] T.C. Lee, K.T. Song, C.H. Lee, C.C. Teng, Tracking control of unicycle-modelled mobile robots using a saturation feedback controller, IEEE Transactions on Control Systems Technology 9 (2) (2001) 305–318.
[9] K.D. Do, Z.P. Jiang, J. Pan, A global output-feedback controller for simultaneous tracking and stabilization of unicycle-type mobile robots, IEEE Transactions on Robotics and Automation 20 (3) (2004) 589–594.
[10] K.D. Do, Z.P. Jiang, J. Pan, Simultaneous stabilization and tracking control of mobile robots: an adaptive approach, IEEE Transactions on Automatic Control 49 (7) (2004) 1147–1151.
[11] S. Blazie, A novel trajectory-tracking control law for wheeled mobile robots, Robotics and Autonomous Systems 59 (2011) 1001–1007.
[12] R. Sepulchre, M. Jankovic, P. Kokotovic, Constructive Nonlinear Control, Springer, New York, 1997.
[13] W. Dixon, D. Dawson, F. Zhang, E. Zergeroglu, Global exponential tracking control of mobile robot system via a PE condition, IEEE Transactions on Systems Man and Cybernetics, B 30 (1) (2000) 129–142.
[14] W.E. Dixon, D.M. Dawson, E. Zergeroglu, Nonlinear Control of Wheeled Mobile Robots, Springer-Verlag, London, 2001.
[15] W.E. Dixon, M.S. de Queiroz, D.M. Dawson, T.J. Flynn, Adaptive tracking and regulation of a wheeled mobile robot with controller/update law modularity, IEEE Transactions on Control Systems Technology 12 (1) (2004) 138–147.
[16] K.D. Do, J. Pan, Global output-feedback path tracking of unicycle-type mobile robots, Robotics and Computer-Integrated Manufacturing 22 (2) (2006) 166–179.
[17] I. Zohar, A. Ailon, R. Rabinovici, Mobile robot characterized by dynamic and kinematic equations and actuator dynamics: trajectory tracking and related application, Robotics and Autonomous Systems 59 (2011) 343–353.
[18] M. Krstic, I. Kanellakopoulos, P. Kokotovic, Nonlinear and Adaptive Control Design, Wiley, New York, 1995.
[19] H. Khalil, Nonlinear Systems, Prentice Hall, 2002.
[20] F. Mazen, A. Iggidr, Backstepping with bounded feedbacks, Systems & Control Letters 51 (3–4) (2004) 235–245.
[21] T. Fukao, H. Nakagawa, N. Adachi, Adaptive tracking control of a nonholonomic mobile robot, IEEE Transactions on Robotics and Automation 16 (5) (2000) 609–615.
[22] A.M. Bloch, M. Reyhanoglu, N.H. McClamroch, Control and stabilization of nonholonomic dynamic systems, IEEE Transactions on Automatic Control 37 (11) (1992) 1746–1757.
[23] R. Fierro, F.L. Lewis, Control of a nonholonomic mobile robot: backstepping kinematics into dynamics, in: Proceedings of the 34th IEEE Conference on Decision and Control, 1995, pp. 3805–3810.
[24] N. Marchand, A. Hably, Global stabilization of multiple integrators with bounded controls, Automatica 41 (12) (2005) 2147–2152.
[25] Z. Lin, Global control of linear systems with saturating actuators, Automatica 34 (7) (1998) 897–905.
[26] A.R. Teel, Global stabilization and restricted tracking for multiple integrators with bounded control, Systems and Control Letters 18 (3) (1992) 165–171.
[27] K.D. Do, J. Pan, Underactuated ships follow smooth paths with integral actions and without velocity measurements for feedback: theory and experiments, IEEE Transactions on Control Systems Technology 14 (2) (2006) 308–322.
[28] K.D. Do, J. Pan, Control of Ships and Underwater Vehicles: Design for Underactuated and Nonlinear Marine Systems, Springer, 2009.

Khac Duc Do received his M.E. and Ph.D. degrees (with Distinction) in mechanical engineering from The University of Wollongong, Wollongong, Australia, and The University of Western Australia, Crawley, Australia, in 1999 and 2003, respectively. Before 2012, he was a Research Professor with the School of Mechanical Engineering, The University of Western Australia. He is currently an Associate Professor with the Department of Mechanical Engineering, Curtin University of Technology. He has published more than 50 articles in peer-reviewed journals and two monographs. His research interests include control of nonlinear systems, control of multiple agents, control of land, air, and ocean vehicles, and control of systems governed by partial differential equations.